Westinghouse Non-Proprietary Class 3

WCAP-16943-NP

June 2008

Enhanced GRCA Rodlet Design

Westinghouse

Enhanced GRCA Rodlet Design

June 2008

Authors:

M. E. Conner
M. J. Hone
J. Long
R. Pomirleanu
G. Wikmark

Prepared by:
R. Knott*
M. J. Riggs*

Approved by:
T. Rodack*

*** Electronically Approved Records Are Authenticated in the Electronic Document Management System**

Westinghouse Electric Company LLC
4350 Northern Pike
Monroeville, PA 15146

© 2008 Westinghouse Electric Company LLC
All Rights Reserved

This page intentionally left blank

Table of Contents
Enhanced GRCA Rodlet Design

Section	Title	Page
1.0	**Purpose and Summary**	**1**
1.1	Purpose	1
1.2	SRP 4.2 Acceptance Criteria Road Map	1
1.3	Summary	4
2.0	**Design Description of Enhanced GRCAs**	**5**
2.1	Overall GRCA Design Considerations	5
2.2	Tungsten GRCA Rodlet Design	6
3.0	**Nuclear Design Considerations**	**8**
3.1	Methodology	8
3.2	GRCA Reactivity Control Function	8
3.3	GRCA Effect on Power Distribution	10
3.4	Predicted Neutron Fluences and Transmutation in the Enhanced Tungsten GRCA	12
3.5	Treatment of Tungsten GRCAs in Safety-Related Nuclear Design Analysis for AP1000	15
3.6	Description and Benchmarking of Nuclear Methods for Tungsten GRCAs	15
3.7	Summary of Nuclear Design Considerations	19
4.0	**Material Properties of Tungsten**	**20**
4.1	**Physical Properties**	**20**
4.1.1	Physical Properties of Unirradiated Tungsten	20
4.1.2	Thermal Expansion	21
4.1.3	Specific Heat	21
4.1.4	Thermal Conductivity	22
4.2	**Mechanical Properties**	**23**
4.2.1	Elastic Properties	23
4.2.2	Tensile Properties	23
4.2.3	Hardness	24
4.2.4	Phase diagram, Re-W	25
4.3	**Compatability with Reactor Coolant**	**26**
4.3.1	Corrosion by Water and Steam	26

Table of Contents
Enhanced GRCA Rodlet Design
(continued)

Section	Title	Page
4.4	**Material Irradiation Experience**	28
4.4.1	Tungsten Irradiation Experience	28
4.4.2	Irradiation Effects on Materials	28
4.4.3	Irradiation Effects in Tungsten	29
4.4.4	Expected Limiting Fluences	31
4.4.5	Impact of Irradiation	31
4.4.5.1	Mechanical Impact on Tungsten due to Irradiation	31
4.4.5.2	Swelling of Tungsten due to Irradiation	32
4.4.5.3	Tungsten Swelling from Transmutation	34
4.4.6	Summary of Material Property Impacts	35
5.0	**Design Bases and Evaluations**	36
5.1	**Nuclear Design**	36
5.1.1	GRCA Reactivity Worth	36
5.1.2	GRCA Effect on Power Distribution	36
5.2	**Mechanical Design Bases and Evaluations**	37
5.2.1	Internal Pressure and Cladding Stresses during Normal, Transient, and Accident Conditions	37
5.2.2	Irradiation Stability of the Absorber Material, Taking into Consideration Gas Release and Swelling	37
5.2.3	Absorber Material Swelling	38
5.2.4	Potential for Interaction Between the Absorber and the Coolant	38
5.3	**Thermal and Hydraulic Design Bases and Evaluation**	38
5.3.1	Maximum Absorber Temperature	39
5.3.2	No Surface Boiling within the Dashpot Region	39
5.3.3	No Bulk Boiling in the Guide Thimble Tubes	40
5.3.4	Bypass Flow in Guide Thimble Tubes	40
5.4	**Summary**	41

Table of Contents
Enhanced GRCA Rodlet Design
(continued)

Section	Title	Page
6.0	Post-LOCA Survivability	42
7.0	Operational Monitoring Program	44
8.0	References	45

This page intentionally left blank

List of Tables
Enhanced GRCA Rodlet Design

Table	Title	Page
1.0-1	Standard Review Plan Section 4.2, Subsection II – Acceptance Criteria	3
2.1-1	Comparison of Overall Interface Characteristics of GRCA Design with RCCA Design	6
3.4-1	Maximum Predicted Absorber Fluence Accumulations (Neutrons/Cm^2) for Tungsten GRCA on the Absorber Surface	12
3.6-1	PARAGON vs. MCNP Benchmark Results for Eigenvalue and GRCA Worth	19
4.1-1	Specific Heat	21
4.1-2	Thermal Conductivity	22
4.2-1	Elastic Properties, Polycrystalline Tungsten	23
4.4-1	Irradiations of Tungsten and Tungsten Alloys	30

This page intentionally left blank

List of Figures
Enhanced GRCA Rodlet Design

Figure	Title	Page
2.2-1	Cross Section Views of Enhanced GRCA Rodlet	7
3.2-1	Comparison of Enhanced GRCA Rod Worth Variation Due to Absorber Depletion	10
3.3-1	Comparison of Representative GRCA Rodded Pin Power Distributions for 1/8 Assembly Geometry, and Change in Pin Power During GRCA Removal	11
3.4-1	Predicted Average Transmutation of Tungsten Absorber	13
3.4-2	Predicted Outer Surface Transmutation of Tungsten Absorber	14
4.2-1	Tensile Properties	23
4.2-2	Hardness	24
4.2-3	Phase diagram, Re-W	25
4.3-1	Corrosion Of Various Tungsten Alloys In High Temperature Water	27
4.4-1	Swelling of Tungsten and W-25%Re	33
6.0-1	Tungsten-Nickel Phase Diagram	42
6.0-2	Tungsten-Iron Phase Diagram	43

This page intentionally left blank

Enhanced GRCA Rodlet Design

1.0 Purpose and Summary

1.1 Purpose

This topical report presents generic design and evaluation information for the introduction of an enhanced Gray Rod Cluster Assembly (GRCA) absorber rodlet by substituting tungsten (W) as the neutron absorber material in lieu of silver-indium-cadmium (Ag-In-Cd) for use in the current NRC approved GRCA design for the AP1000 reactor plant.

This report describes the basic absorber rodlet design using tungsten in a reduced worth control rod, i.e. GRCA. The focus of this topical and the accompanying evaluations is directed at the replacement tungsten absorber material that is internal and double encapsulated in the absorber rodlet, since the basic reduced worth control rod cluster design (i.e., outer rodlet diameter and other overall interface dimensions) remains the same as the previously NRC reviewed and approved GRCA design described in the AP1000 Design Control Document (DCD) (References 1 and 2). This topical report provides the proposed licensing basis for evaluating the enhanced GRCA design and, when approved, will serve as the basis for application of the enhanced GRCA rodlet design.

GRCAs using reduced worth control rods have been approved for use in the AP1000 and other nuclear reactor plants around the world. The introduction of tungsten as a low worth control rodlet absorber will enhance the mechanical and nuclear performance of a low worth control rod (i.e., increased lifetime and constant reactivity) relative to the standard Ag-In-Cd absorber. Tungsten control rodlets can be designed to match the existing NRC approved reduced worth control rods and as a result would not affect the operational characteristics of a reactor core using GRCAs.

1.2 SRP 4.2 Acceptance Criteria Road Map

NUREG 0800 Standard Review Plan (SRP) Section 4.2, "Fuel System Design," (Reference 8) provides the principal guidance that has been used for evaluating the acceptability of the enhanced GRCA reactivity control rod/rodlet design for use in the AP1000 reactor core. In the AP1000 DCD, the overall GRCA design was shown to meet the required design bases and limits in accordance with the Standard Review Plan. As stated in Section 1.1, the purpose of this topical report is to discuss changes in the GRCA rodlet design to incorporate the use of tungsten as the absorber material for the enhanced GRCA design instead of Ag-In-Cd. As such the focus of this report is directed at those aspects of the GRCA design, specifically the rodlet itself, that are impacted by this change. Other aspects of the GRCA design that are not impacted by the absorber material change and were already considered in the DCD will not be addressed in this report.

Section II.1.A.viii of the SRP discusses considerations for changes in control rod design. Specifically, the following items are indicated for review:

1. Changes in control rod configuration
2. Introduction of new materials
3. Changes in neutronics and mechanical lifetime
4. Changes in mechanical design
5. The ability to exclude water/coolant if water-soluble or leachable materials are used

All of these items are specifically addressed in this report. In addition, the specific criteria that are related to the rodlet design changes are addressed in the evaluations of the appropriate design bases.

The report is organized to cover the key SRP areas of design bases, design description, design evaluation, and testing inspection, and surveillance plans as follows:

Section 2.0 - Overall Design Description

Section 3.0 - Nuclear Design Description (which also includes an evaluation of analytical prediction capability)

Section 4.0 - New Material Property Description (including significant irradiation experience with tungsten)

Section 5.0 - Design Bases and Evaluation (Nuclear, Mechanical, and Thermal/Hydraulic)

Section 6.0 - Post-LOCA Survivability

Section 7.0 - Operational Monitoring Program

Based on a thorough review of the SRP 4.2 guidance, the following Table 1.0-1 presents an overview of the SRP acceptance criteria addressed for the introduction of the enhanced GRCA rodlet design, and the corresponding section(s) of the topical report in which the SRP criteria is addressed.

TABLE 1.0-1
STANDARD REVIEW PLAN SECTION 4.2
SUBSECTION II. - ACCEPTANCE CRITERIA

		SRP Subsection	Topical Report Section
Design Bases	Fuel System Damage	II.1.A.i. - Stress, Strain or Loading Limits on grids, GT, thimbles, fuel rods, control rods & other fuel system structural members	5.2, 5.3
		II.1.A.viii. (1) - Changes in control rod configuration	2.2
		II.1.A.viii. (2) - Introduction of new materials	4.1, 4.2, 4.3, 4.4, 4.5
		II.1.A.viii. (3) - Changes in neutronics and mechanical lifetime	5.1, 5.2
		II.1.A.viii. (4) - Changes in mechanical design	2.1, 2.2, 5.2, 5.3
		II.1.A.viii. (5) - The ability to exclude water/coolant if water-soluble or leachable materials are used.	4.3
Description & Design		II.2. Description & Design	2.0, 3.0, 4.0
Design Evaluation		II.3.C. - Analytical Prediction	3.1, 3.2, 3.3, 3.4, 3.6
Testing, Inspection and Surveillance Plans		II.3.D. - Test, Inspections, Surveillance	7.0

1.3 Summary

a. The results of the Mechanical Design evaluation performed for the enhanced GRCA rodlet design confirm that the design will perform its intended function and that the design bases are satisified.

b. The results of the Nuclear Design evaluation performed for the enhanced Gray Rod Cluster Assembly design confirm that:

- Standard nuclear design analytical models and methods accurately describe the neutronic behavior of the enhanced GRCA design.
- The enhanced GRCA nuclear design bases are satisfied.

c. The results of the Thermal and Hydraulic Design evaluation for the enhanced GRCA rodlet design confirm that the design bases are satisfied.

d. The evaluation of materials data available for the tungsten absorber material confirm that:

- Material properties of tungsten are understood and well documented such that appropriate design evaluations can be made.
- Significant irradiation experience exists such that the impacts of irradiation on key design characteristics can be assessed for AP1000 operating conditions.

2.0 Design Description of Enhanced GRCAs

2.1 Overall GRCA Design Considerations

Low worth Gray Rod Cluster Assemblies (GRCAs) are used in advanced nuclear reactors to provide a mechanical means of making relatively small adjustments in core reactivity. The use of GRCAs to mechanically adjust (or "shim") the core reactivity reduces the need to make small adjustments to the soluble boron concentration in the reactor coolant using the Chemical and Volume Control System (CVS). This reduces waste water processing required on a daily basis, and allows for simplification of the CVS design and operation. GRCAs are automatically repositioned as necessary to maintain a programmed average coolant temperature during baseload and load follow operation. The movement of GRCAs effectively compensates for reactivity effects due to fuel and burnable absorber depletion, power and temperature changes, and changes in the core xenon condition.

The reactivity control function of low worth GRCAs should be clearly distinguished from that of high worth, or black Rod Control Cluster Assemblies (RCCAs), which are primarily intended to provide rapid shutdown capability for the reactor core. GRCAs are dropped into the core during a reactor trip, but the negative reactivity associated with their insertion is small in comparison to the total negative reactivity available from the RCCAs, and is not needed to safely shut down the reactor. Therefore, GRCAs as considered in this report perform an operational reactivity control function, but are not required for shutdown as the result of a reactor trip.

The basic overall design of the enhanced GRCAs and current GRCAs, as well as RCCAs, is the same except for the absorber design in the inside of the absorber rodlets. The overall outline dimensions as well as the interfaces with the control rod drive mechanisms and the fuel assembly and guide thimbles are identical. In the case of the enhanced GRCAs and RCCAs, there are twenty four rodlets attached to a spider assembly that is attached to the control rod drive mechanism. The outer diameter of the rodlets of the enhanced GRCA and current RCCA/GRCA designs is identical. Table 2.1-1 show a comparison of key interface parameters of the GRCA and RCCA designs.

Table 2.1-1
COMPARISON OF OVERALL INTERFACE CHARACTERISTICS OF GRCA DESIGN WITH RCCA DESIGN

	RCCA (DCD R.16)	GRCA	
		Enhanced GRCA	DCD R.16
Rodlet O.D. (in.)	0.381	0.381	0.381
Overall Assembly Length	Same	Same	Same
Spider Design	Same	Same	Same
No. of Rodlets	24	24	12 SS / 12 Ag-In-Cd
Absorber Material	Ag-In-Cd	Tungsten (W)	Ag-In-Cd

2.2 Tungsten GRCA Rodlet Design

Figure 2.2-1 illustrates the Enhanced GRCA rodlet design. GRCA rodlets have an outside stainless steel cladding with top and bottom end plugs nearly identical to those of current RCCA rodlets.

Inside the cladding, the tungsten material of circular cross-section is further enclosed in a sleeve, which is sealed at the top and bottom. Thus, the tungsten absorber is double encapsulated. [

]^{a,c} The space between the cladding and sleeve is backfilled with an inert gas. The sleeve is held in place by a holddown device.

It should be noted that with the tungsten absorber, due to the optimum worth of this absorber material for GRCA application in the AP1000, all 24 rodlets attached to the spider are identical absorber rodlets. This compares with the GRCA design described in DCD Rev. 16, where only twelve of the 24 rodlets are absorber rodlets with a reduced diameter Ag-In-Cd absorber and the other 12 rodlets are inert stainless steel rodlets.

[ ] a,c

FIGURE 2.2-1 CROSS SECTION VIEWS OF ENHANCED GRCA RODLET

3.0 Nuclear Design Considerations

3.1 Methodology

Nuclear design calculations for GRCAs using tungsten as the absorber material are based on unit assembly results and homogenized group cross sections generated by the PARAGON lattice code (Reference 3). The PARAGON code is capable of accurately modeling the tungsten GRCAs. PARAGON is a two-dimensional neutron transport theory code that is typically used to model single or multi-assembly lattice calculations, including the presence of control rod assemblies when appropriate. The PARAGON 70-group neutron cross section library was updated to include appropriate tungsten and rhenium nuclide cross section data from ENDF/B-VI.8, using the same methodology described in Reference 3. Benchmarking of PARAGON against the industry standard MCNP code has been performed. An independent research effort by Rensselaer Polytechnic Institute (RPI) has also confirmed the accuracy of the ENDF/B-VI neutron capture and total cross sections for tungsten. More details regarding the ability of PARAGON to accurately model the tungsten GRCA are included in Section 3.6 of this report.

3.2 GRCA Reactivity Control Function

The targeted rod worth for GRCAs in a given plant design is dependent on the intended operating strategy for the plant, the kinetic characteristics of the reactor core, and the control rod pattern. The specific example discussed in this report is a GRCA design for the Westinghouse AP1000 reactor (Reference 1), which uses 16 GRCAs in the control rod pattern. The AP1000 plant is designed to be capable of performing many types of load follow maneuvers without requiring a change in the core soluble boron concentration during the maneuver. For AP1000, this targeted operational capability is the most limiting factor defining the minimum rod worth needed from the GRCAs. The maximum rod worth of GRCAs is not strictly limited, but GRCA designs that provide significantly more rod worth than required can affect the core power distribution more than necessary, as discussed in Section 3.3. Ideally, the GRCA rod worth should be maintained within a relatively narrow band about the optimum worth, in order to provide the intended control capability with minimal effect on power distribution. The tungsten based GRCA design described in Section 2.0 has been confirmed to meet the intended GRCA rod worth target for the AP1000 reactor, as described below.

The rod worth of each individual GRCA or bank of GRCAs will vary, depending on the core location, time in life, and fuel loading pattern of the core. Therefore, in order to allow for valid comparisons, GRCA rod worth has been studied on a relative basis, using single unit assembly geometry calculations performed with the PARAGON transport theory lattice code. Unit assembly rod worth calculations performed for the enhanced GRCA rodlet design were compared to the results of identical calculations for a reference GRCA design that is known to meet the required rod worth for AP1000. These calculations included modeling depletion of the GRCA absorber material for a neutron fluence equivalent to

approximately 20 years of service in the AP1000 reactor.

The AP1000 reactor was initially designed to utilize GRCAs with four standard Silver-Indium-Cadmium (Ag-In-Cd) black absorber rodlets in each GRCA component, and was approved on that basis (Reference 1). The four rodlet Ag-In-Cd GRCA design was originally confirmed to provide the correct total GRCA rod worth needed to achieve the intended load follow capability for AP1000, without changing the soluble boron concentration. This GRCA design is thus considered the reference design, and was modeled in unit assembly geometry to establish the reference target rod worth for subsequent comparisons. Sensitivity studies were also performed on the reference design to determine how much GRCA worth could be allowed to decrease before boron concentration changes would become necessary to perform some of the required load follow sequences. While loss of the intended load follow capability would not cause any safety concerns or prevent continued baseload operation of the reactor, it could result in more complexity of operations and more waste water generation if a large load change maneuver became necessary when there is insufficient GRCA worth. The minimum acceptable GRCA rod worth established from the sensitivity studies was determined to be [ ]^{a,c} of the initial undepleted reference worth. This was used to establish the lower limit on GRCA worth, corresponding to the end of useful life time.

In Reference 2, an improved Ag-In-Cd based GRCA design was defined for the AP1000. The revised design reduced the Ag-In-Cd absorber diameter within each rodlet and spread the absorber material out among 12 of the 24 available rodlets in the control assembly. This change significantly improved the local pin power distribution characteristics for rodded operation and met the required GRCA rod worth. However, because of the high fluence accumulation rates associated with gray rod operation and the natural depletion characteristics of the absorber material, neither Ag-In-Cd GRCA design is capable of maintaining the minimum [ ]^{a,c} targeted reference rod worth for the desired service life time.

The enhanced GRCA rodlet design described in this report replaces the Ag-In-Cd primary absorber material with commercially pure tungsten. Tungsten has a significantly lower total neutron absorption cross section than Ag-In-Cd, which results in a naturally slower absorber depletion rate. In addition, the depletion of tungsten leads to the formation of ^{187}Re, which is a slightly stronger neutron absorber than natural tungsten. Over the life time of a tungsten GRCA, the buildup of ^{187}Re more than compensates for the depletion of the tungsten absorber nuclides. The result is that the rod worth of a tungsten GRCA will have a slightly increasing, but nearly flat trend with long term neutron exposure due to ^{187}Re buildup. This is illustrated in Figure 3.2-1, which plots the unit assembly GRCA rod worth for tungsten and both Ag-In-Cd GRCA designs discussed above at various stages of depletion during their life time. Figure 3.2-1 also shows the optimum targeted GRCA rod worth specific to AP1000, and the [ ]^{a,c} rod worth corresponding to the end of useful life time, when the ability to load follow without changing the soluble boron concentration can no longer be demonstrated for all intended scenarios. As shown in Figure 3.2-1, the overall change in rod worth for a tungsten GRCA is significantly smaller than the decrease in rod worth predicted for a similar period of depletion for both Ag-In-Cd GRCA designs. This relatively flat depletion worth characteristic of tungsten makes possible GRCA designs that utilize a minimum amount of absorber material in all 24 rodlets of the control assembly, without having any adverse effects on the

GRCA useful life time. A further expected benefit of the relatively flat depletion worth characteristic for tungsten is that it minimizes the potential for long term formation of undesirable axial gradients in the GRCA absorber strength, which could also limit useful life time.

Figure 3.2-1 demonstrates that the AP1000 GRCA targeted rod worth requirement can be met with the enhanced tungsten based GRCA design, and that absorber depletion effects will not limit the useful service life time of the component.

[ ] a,c

FIGURE 3.2-1 COMPARISON OF ENHANCED GRCA ROD WORTH VARIATION DUE TO ABSORBER DEPLETION

3.3 GRCA Effect on Power Distribution

Power distribution effects from GRCA operation are minimized by minimizing the rod worth of the GRCAs, and by evenly distributing the absorber material in the GRCA to the maximum extent possible.

Figure 3.2-1 demonstrates that the tungsten based GRCA design matches the optimum targeted GRCA rod worth for AP1000 very closely. The relatively flat depletion worth curve for the tungsten design allows for a long service life time without requiring that additional rod worth be built into the design to account for absorber depletion effects. The ability to use the minimum required GRCA rod worth minimizes the potential increase in peaking factors from flux redistribution in other unrodded core

locations when a GRCA bank is fully inserted. This allows core designs to be better optimized, while still maintaining the full power operating capability. AP1000 cores are designed to meet peaking factor limits with allowed GRCA insertion, and will be monitored on-line to ensure that the limits are met at all times.

Evenly distributing the GRCA absorber material among all 24 absorber rodlets minimizes the effect of GRCA operation on the local pin power distribution in the assembly containing the GRCA. This is illustrated in Figure 3.3-1, which shows representative rodded pin power distributions for the various Ag-In-Cd and tungsten GRCA designs in single assembly calculations, and shows the predicted change in local pin power when changing from a rodded to unrodded configuration. Figure 3.3-1 presents the assembly rodded pin power distributions for only 1/8 of the assembly for simplicity, since the assembly used in the model is fully symmetric in this geometry. Figure 3.3-1 also illustrates the relative position of the GRCA absorber rodlets in the guide thimbles for each calculation and the relative blackness to neutrons of each GRCA rodlet design. The results clearly demonstrate that the use of 24 gray absorber rodlets minimizes the effect of GRCA operation on the local pin power distribution of the rodded assembly.

a,c

FIGURE 3.3-1 COMPARISON OF REPRESENTATIVE GRCA RODDED PIN POWER DISTRIBUTIONS FOR 1/8 ASSEMBLY GEOMETRY, AND CHANGE IN PIN POWER DURING GRCA REMOVAL

3.4 Predicted Neutron Fluences and Transmutation in the Enhanced Tungsten GRCA

The tungsten GRCA design has been simulated and depleted under a neutron fluence equivalent to [ ]^{a,c}, using the PARAGON code. PARAGON performs a 70-group neutron transport theory calculation, and through the use of representative fuel and thermal conditions, correctly captures the average intensity and energy spectrum of the neutron flux expected in the AP1000 reactor. As described in Section 3.6, PARAGON has been modified to be capable of depleting a tungsten neutron absorber rodlet. The PARAGON depletion calculations are roughly equivalent to [ ]^{a,c}. This assumption is consistent with the intended operating strategy for GRCAs in AP1000. The resulting maximum predicted absorber fluences for the simulated operation are shown in Table 3.4-1. The maximum predicted fluences are described in terms of the applicable neutron energy range, in order to allow for comparison with published irradiation data on tungsten. Results are presented for only the outer surface of the tungsten absorber, which accumulates the highest fluence. Thermal and resonance energy self shielding effects reduce the fluence in the interior of the tungsten absorber below that of the surface.

Figure 3.4-1 illustrates graphically how the tungsten absorber nuclide concentrations are predicted to change over the simulated operating fluence. This figure represents the average nuclide concentration and total fluence over the entire absorber zone. Figure 3.4-2 presents similar results for the outer surface of the tungsten absorber. Transmutation effects are slightly larger on the absorber surface due to self shielding effects.

TABLE 3.4-1 MAXIMUM PREDICTED ABSORBER FLUENCE ACCUMULATIONS (NEUTRONS/CM^2) FOR TUNGSTEN GRCA ON THE ABSORBER SURFACE

[ ] a,c

a,c

FIGURE 3.4-1 PREDICTED AVERAGE TRANSMUTATION OF TUNGSTEN ABSORBER

a,c

[ ]

FIGURE 3.4-2 PREDICTED OUTER SURFACE TRANSMUTATION OF TUNGSTEN ABSORBER

3.5 Treatment of Tungsten GRCAs in Safety-Related Nuclear Design Analysis for AP1000

Westinghouse nuclear design models for AP1000 cores containing tungsten GRCAs will include the GRCAs in the model, and predictions of the GRCA rod worth and core operating characteristics will be made in advance of core operation. However, Westinghouse intends to exclude crediting negative reactivity insertion from tungsten GRCAs during analytical shutdown margin calculations made prior to the startup of the core. Therefore, the pre-operation analysis will confirm that there is sufficient margin to shut down the reactor without crediting any negative reactivity insertion from GRCAs falling into the core. It is expected, however, that when the reactor is in a shut down or hot standby condition with GRCA banks confirmed to be inserted by position indication, that utility and Westinghouse personnel may credit the presence of the inserted GRCAs for any shutdown margin or shutdown boron calculations made subsequent to startup physics testing for the cycle, providing that the total measured GRCA rod worth has been confirmed to meet the physics testing acceptance criteria.

Other analytical calculations that involve modeling the insertion of GRCAs (e.g., steam line break) will be performed in the most conservative manner, assuming either that the gray rods insert normally or do not insert at all. If the results from an analytical calculation are sensitive to the ability to predict GRCA worth, then a conservative allowance will be included in the predicted GRCA worth within the analysis, consistent with the review criteria established for GRCA bank worth during startup physics testing. Peaking factor uncertainties will not be changed. Typical GRCA banks have reactivity worths that are [ ]^{a,c}. The effect on core peaking factors associated with GRCA movement is therefore naturally smaller than for allowed RCCA movement, and core peaking factors are continuously monitored in AP1000 with the BEACON™ direct margin monitoring system.

3.6 Description and Benchmarking of Nuclear Methods for Tungsten GRCAs

GRCAs containing tungsten as the primary absorber material can be accurately modeled with the Westinghouse PARAGON lattice code. PARAGON is a two-dimensional neutron transport theory code that is typically used at Westinghouse to model single or multi-assembly lattice calculations, including the presence of control rod assemblies when appropriate. PARAGON includes a resonance self shielding model that correctly captures the effect of self shielding on cross sections for materials which have large resonance absorption peaks (e.g., both tungsten and silver are in this category). PARAGON is also capable of depleting fuel and control rod absorber nuclides within the calculated flux environment. Results available from PARAGON include eigenvalues, pin power distributions, fluxes in up to 70 energy groups, reaction rates, depleted number densities, and collapsed group constants that are used in courser mesh nodal models such as the Westinghouse ANC code (Reference 4). ANC is typically used to model the core in 3-dimensions and 2 energy groups, and includes a control rod insertion model that implements cross section modifiers, which are based on comparisons of rodded and unrodded results from the PARAGON lattice code.

In preparation for modeling tungsten based GRCAs in PARAGON, preliminary studies of the depletion characteristics of tungsten were made using the industry standard generalized depletion code ORIGEN (Reference 5). ORIGEN was used to simulate depletion of a gram of pure tungsten in a representative neutron flux for the [ ]^{a,c}. ORIGEN is also capable of predicting gas generation in tungsten from n-p or n-α reactions. The results from ORIGEN indicated that total gas generation in tungsten is very low, and is expected to be less than 0.1 appm for a fluence [ ]^{a,c}. Based on the isotopic content predicted by ORIGEN after this time period, and also a review of the basic neutron cross sections of the various isotopes, the following dominant nuclear reactions were identified for tungsten depletion:

$^{182}W + n \rightarrow$ $^{183}W + n \rightarrow$ ^{184}W

$^{186}W + n \rightarrow$ $^{187}W \rightarrow$ ^{187}Re (after beta decay)

$^{187}Re + n \rightarrow$ $^{188}Re \rightarrow$ ^{188}Os (after beta decay)

The PARAGON 70-group neutron cross section library was updated to include appropriate tungsten and rhenium nuclide cross section data from ENDF/B-VI.8, using the same methodology described in Reference 3. In addition, depletion chains for tungsten were added to PARAGON in order to enable detailed absorber depletion studies. The PARAGON tungsten depletion chains enable tracking specific nuclide concentrations for ^{182}W, ^{183}W, ^{184}W, ^{186}W, and ^{187}Re, as these are the nuclides that are predicted by ORIGEN to be present in abundance in depleted tungsten. ^{187}W, ^{188}Re, and ^{188}Os are not explicitly tracked in PARAGON, either because their abundance was predicted to be very low by ORIGEN, or because they are not significant contributors to the total absorption rate. Figure 3.4-1 shows the PARAGON average predicted transmutation occurring in a tungsten GRCA over a fluence equivalent to [ ]^{a,c}. It should be noted that the total fluence reached on this figure includes all neutron energies from 0-10 MeV, and is representative of the maximum fluence that will be accumulated in a GRCA absorber in service [ ]^{a,c}, after accounting for the intended operating strategy and GRCA shuffling scheme between cycles.

PARAGON modeling methods for tungsten GRCAs were benchmarked against the industry standard Monte-Carlo code MCNP (Reference 6). This is similar to the benchmark calculations performed initially for PARAGON in Reference 3. Specifically, identical single assembly benchmark calculations were performed using both codes at hot and cold temperature conditions, for configurations with and without inserted tungsten GRCAs. Furthermore, the configurations with inserted GRCAs were simulated assuming both fresh and depleted tungsten absorber isotopics. The depleted tungsten calculations included the effects of ^{187}Re buildup representative of [ ]^{a,c}. The results of the benchmark calculations are summarized in Table 3.6-1, and are presented both in terms of an absolute eigenvalue comparison and a GRCA rod worth comparison. The results presented in Table 3.6-1 provide independent confirmation that the PARAGON code has implemented the tungsten cross sections correctly and can predict tungsten GRCA worth with an accuracy comparable to that of black neutron absorbers like Ag-In-Cd, regardless of temperature or absorber depletion state. Therefore, it is expected that tungsten GRCA rod worths predicted by nodal core models using

PARAGON to generate the homogenized few group constants, will be accurate to within the same level of uncertainty as current black control rod designs.

Each MCNP benchmark comparison case was also compared for pin-by-pin power distribution results. The results indicate that PARAGON is capable of matching the MCNP rodded pin powers to within +/- 1%, which is similar to results that have been obtained in benchmark comparisons performed for other types of control rods.

In addition to benchmarking PARAGON against the industry standard MCNP code as discussed above, Westinghouse has identified a published research effort (Reference 7) conducted in 1997 by Rensselaer Polytechnic Institute (RPI) that confirmed acceptable accuracy of the neutron capture and total cross sections for natural tungsten that are currently in the ENDF/B-VI database. In particular, the independent measurements of tungsten performed in 1997 were made using three separate measurement techniques (transmission, capture, and self indication) over the thermal and epithermal neutron energy range that is of most interest to this application of tungsten (0.01 eV to 200 eV). The thermal capture cross section for natural tungsten at 0.0253 eV was reported as 17.09+/- 0.14 barns by RPI, compared to the ENDF/B-VI value of 18.19 barns. The resonance integral was reported as 384 barns by RPI, compared to the ENDF/B-VI value of 360 barns. The differences in the two reported numeric values are both approximately 6-7% and in opposing directions. The RPI study also included plots comparing the ENDF/B-VI capture cross section data to the independently measured capture cross sections, as a continuous function of neutron energy. The plots indicated only very minor differences between the RPI measurements and the ENDF/B-VI database for natural tungsten as a function of energy. In particular, the plotted capture cross sections demonstrated excellent agreement at the energy of the peak thermal neutron flux in the AP1000 neutron spectrum (which ocurrs at approximately 0.12 eV) and within the largest resonance absorption peaks for tungsten occurring at approximately 20 eV. The plots confirm that the basic neutron capture cross sections for tungsten in the ENDF/B-VI database contain no obvious gross errors that could significantly affect accuracy in the nuclear models for this application of tungsten. In addition, PARAGON and MCNP benchmark cases were performed using both natural tungsten and individual tungsten nuclides. The results indicated that the predicted worth of a tungsten GRCA is not significantly different depending on whether or not the natural tungsten cross sections or the individual nuclide cross sections are accessed. Furthermore, an investigation of the ENDF/B-VII cross section library confirmed that the capture and total cross sections for individual tungsten nuclides were not modified over the thermal and epithermal energy range of interest for this application. The combination of diverse MCNP benchmarks and basic cross section confirmation minimizes the risk that there will be any significant misprediction of tungsten GRCA worth using PARAGON based core models.

Finally, in the unlikely event there is a misprediction of tungsten gray rod worth outside of the normal physics testing acceptance criteria, the consequences of such a misprediction will be very minor for plants such as the AP1000. Since the gray rods will not have been credited for shutdown margin made during the core analysis before the startup (see Section 3.5), there will be no impact on the core safety evaluation. Operation of the plant will still be possible both in baseload and load follow modes of operation. In baseload operation, the GRCAs are intended to operate in automatic mode to maintain the

core average temperature program. If the GRCA rod worths are mispredicted then the rods may move at slightly different rates while in auto to achieve the reactivity balance, but the temperature signals that feed the control system will be unaffected. If the rate of GRCA motion is different from predictions, this may ultimately affect the frequency of soluble boron adjustments slightly, but the effects of the misprediction on base load operation will otherwise be unnoticeable. On-line core monitoring will continue to confirm that peaking factor limits are met when the GRCAs are inserted. In load follow operation, if the actual GRCA worth is significantly less than the predicted worth, it is possible that some extreme load follow maneuvers may require a change in the soluble boron concentration. However, this situation, though inconvenient, is well within the capabilities of the plant. Startup physics testing measurements of GRCA worth will be performed as with other RCCA banks, and will identify any problems in the predicted data, allowing for correction in future cycles.

TABLE 3.6-1 PARAGON VS. MCNP BENCHMARK RESULTS FOR EIGENVALUE AND GRCA WORTH

[ ] a,c

3.7 Summary of Nuclear Design Considerations

1. The PARAGON lattice code is capable of accurately modelling the tungsten GRCA design.
2. The enhanced GRCA meets the GRCA worth requirements for the AP1000 reactor specified in the approved DCD.
3. The flat depletion characteristic of the enhanced GRCA will not limit the GRCA service lifetime.
4. Power distribution effects from GRCA operation are minimized with the enhanced GRCA design by minimizing rod worth and allowing dispersion of the absorber over all 24 rodlet locations.
5. Transmutation effects in the enhanced GRCA are well understood.

4.0 Material Properties of Tungsten

This section addresses both the unirradiated material properties of tungsten as well as the impact of irradiation on key characteristics that could influence the GRCA design performance. Section 4.1 addresses the physical properties, Section 4.2 addresses the mechanical properties, and Section 4.3 addresses the compatibility of tungsten with the reactor coolant. These properties are utilized in the design evaluations discussed in Section 5.0 and can be found in the materials handbooks as referenced.

Section 4.4 addresses the effects of irradiation on tungsten. These effects have been examined in a significant number of studies which include high irradiation fluences. [

]a,c

4.1 Physical Properties

The following representative set of unirradiated physical properties for high purity tungsten is well documented and is provided in the accompanying References.

4.1.1 Physical Properties of Unirradiated Tungsten

Density: 19.254 Mg/m^3 (Ref. 9)
Atomic weight: 183.85 g/mole (Ref. 9)
Melting point: 3410 ± 20°C (Ref. 9); 3380°C (Refs. 11, 15)
Boiling point: 5700 ± 200°C (Ref. 9); 5500°C (Refs. 11, 15)
Crystal structure: Body centered cubic, A2, at all temperatures below the melting point (Refs. 9,11,15)

Based on the above melting point and uncertainty, a minimum absorber melting point of 3380°C is used as a design value.

4.1.2 Thermal Expansion

From 25°C to 2500°C (Reference 9), powder metallurgy rod:

$$\frac{L - L_{25°C}}{L_{25°C}} * 100 = -8.69 * 10^{-3} + 3.83 * 10^{-4} * T_C + 7.92 * 10^{-8} * T_C^{\ 2}$$

4.1.3 Specific Heat

Specific heat (Reference 9), from 0 to 3000°C:

$$c_p = 135.76(1 - 4805T^{-2}) + (9.1159 * 10^{-3})T + (2.3134 * 10^{-9})T^3$$

where c_p is in J kg^{-1} K^{-1} and T is in K

Specific heat (Reference 11):

Table 4.1-1

T, K	C_p, cal K^{-1} g-atom^{-1}	C_p, J K^{-1} kg^{-1}
298.15	5.80	132
400	6.00	137
500	6.12	139
600	6.22	142
700	6.30	143
800	6.37	145
900	6.44	147
1000	6.52	148

Specific heat (Reference 15), 298 – 3000K:

$c_p = 5.69 + 7.8 * 10^{-4}$ T

where c_p is in cal K^{-1} mole^{-1} and T is in K

4.1.4 Thermal Conductivity

Thermal conductivity (Reference 9):

Table 4.1-2

Temperature, °C	P, W $m^{-1}K^{-1}$
0	165
500	135
1000	120
1500	105
2000	95

4.2 Mechanical Properties

4.2.1 Elastic Properties

Elastic Properties, Polycrystalline Tungsten (Reference 9):

Table 4.2-1

Temperature, °C	E, GPa	ν
0	407	0.283
400	393	0.285
800	376	0.289
1200	357	0.295
1600	335	0.300

4.2.2 Tensile Properties

In general, unirradiated tungsten gains ductility and loses strength with increasing temperature.

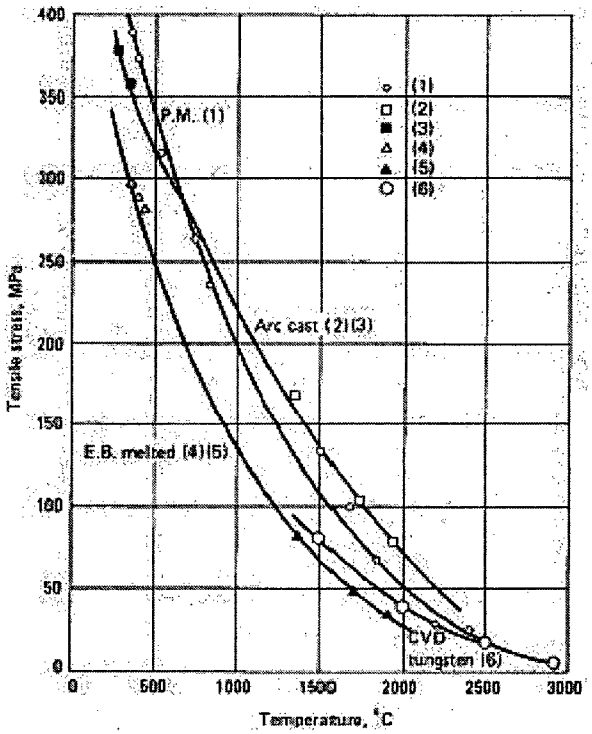

FIGURE 4.2-1 TENSILE PROPERTIES (REFERENCE 9)

4.2.3 Hardness

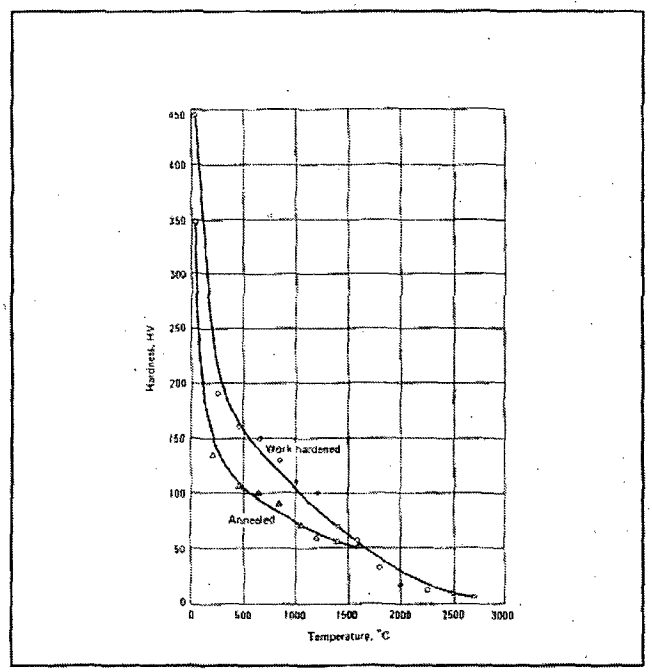

FIGURE 4.2-2 HARDNESS (REFERENCE 9)

4.2.4 Phase diagram, Re-W

Rhenium is formed as tungsten is transmuted.

Phase diagram, Re-W (Reference 12). Tungsten-rhenium alloys remain body-centered-cubic, isotropic with W, at all compositions predicted to form from transmutation in GRCA service.

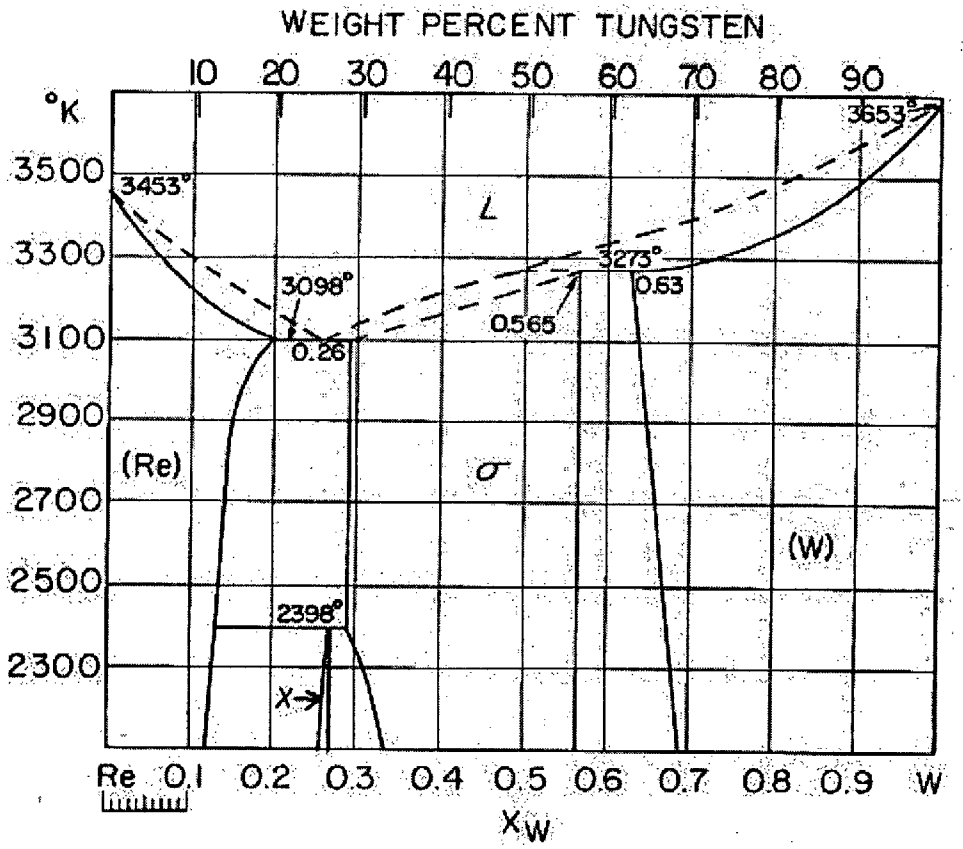

FIGURE 4.2-3 PHASE DIAGRAM, Re-W (REFERENCE 12)

4.3 Compatibility with Reactor Coolant

In the application of tungsten as an absorber in an LWR, the absorber material could possibly come into contact with the reactor coolant in the unlikely event of cladding failure and cause corrosion of the tungsten. For this reason the enhanced GRCA design employs an inner sleeve in addition to the outer cladding to double encapsulate the tungsten, thereby doubly protecting it from the coolant. The coolant conditions involve water of temperatures up to 330°C, with up to 2000 ppm or more of boron, up to 3.5 ppm or more of lithium ions, with up to 4 ppm or more of hydrogen, and corrosion products and impurities at a much lower level, i.e. ppb levels. The pH is maintained between 6.9 and 7.4.

4.3.1 Corrosion by Water and Steam

Tungsten corrodes in contact with air (Ref. 9) and starts forming a thin film of tungsten trioxide at room temperature (Ref. 47). Temperatures above 200°C and humidity will accelerate the corrosion process. The corrosion rate is dependent on the temperature and the oxygen pressure (Ref. 47). The oxide will be protective only to a limited extent. At temperatures above 700°C, the oxide will start sublimating (Ref. 47) with some acceleration in the presence of steam (Refs. 46, 45).

Tungsten reacts slowly in contact with water even at temperatures below 100°C (Ref. 47). The corrosion rate has been reported to be 160 $mg/dm^2/h$ at elevated temperature (150 to 360°C) and higher pressures (70 to 80 atm) (Ref. 47). In a more extensive study, it was found that the corrosion rate in water at elevated temperature is dependent on alloying elements and the metallurgical processing of the tungsten (Ref. 16). Pure tungsten has a lower corrosion rate than tungsten-rhenium alloys, as illustrated in Figure 4.3-1. The negative mass gain values illustrate corrosion product solubility in the water. Only the different forms of tungsten processing, such as polycrystalline (W-P, HPW), single crystal (W-S), CVD formed tungsten, and the various tungsten-rhenium alloys, up to 26% Re (W-26Re) are discussed in this report.

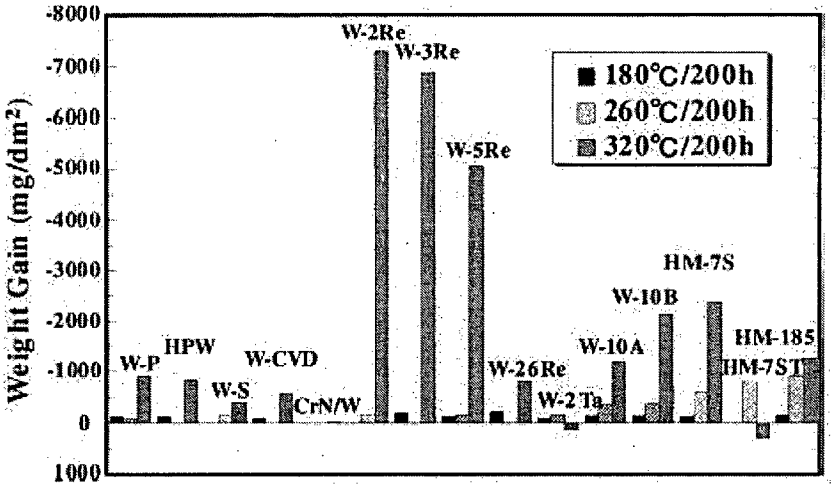

FIGURE 4.3-1 CORROSION OF VARIOUS TUNGSTEN ALLOYS IN HIGH TEMPERATURE WATER (REFERENCE 16).

An alkaline environment will increase the corrosion rate due to the increased solubility of the tungsten trioxide in alkaline environments (Ref. 44).

The density of the formed oxide, WO_3, is considerably lower than for tungsten (Refs. 16, 44) and an oxidation of tungsten by oxygen, air, steam or water would increase the volume of a oxidized body of tungsten.

As described earlier, the enhanced GRCA rodlet design utilizes double encapsulation consisting of an outer clad and inner sleeve to prevent the reactor coolant from coming into contact with the tungsten absorber. Even in the unlikely event of breach of the cladding, the inner sleeve serves to protect the absorber from the coolant.

4.4 Material Irradiation Experience

4.4.1 Tungsten Irradiation Experience

Irradiation effects on tungsten have been studied since 1968 (Refs. 27, 28, 37, 38, 41). The interest in tungsten for nuclear application has evolved since then due to the use or planned use of tungsten in three major fields in the nuclear industry. These fields are space power generation (Refs. 19, 20, 43), spallation neutron source targets (Ref. 22, 29) and more recently and most extensively, for the proposed use of tungsten as armor in the development of fusion power reactors, such as Tokamaks (Refs. 18, 21, 23, 25, 26, 30, 31, 33, 34, 36, 39, 40).

In these applications, the space power generation has generally been limited to rather low neutron fluences, less than $2x10^{21}$ n·cm^{-2} although up to ten times higher fluences are considered in advanced applications (Ref. 19). The studies for the fusion field and the limited studies with regard to spallation sources have been performed at higher fluences, up to $144x10^{21}$ n·cm^{-2} (E>0.1 MeV) (Ref. 30), [

]^{a,c}

4.4.2 General Discussion of Irradiation Effects on Materials

Irradiation effects on solid materials are either microstructural changes due to particle impact or transmutation. Microstructural changes are generally produced by fast neutrons of sufficient impact energy to cause a knock-on effect disturbing the crystal lattice of the material. In reality this means that the fast neutrons must have an energy above 0.1 or 1 MeV to cause such significant impact by forming defect clusters in the material. The effect of the defect cluster formation by each neutron impact in the material is the formation of vacancies and interstitials in the material's crystal structure. Most of the vacancies and interstitials in the cluster recombine resulting in no net effect, but some vacancies and interstitials will remain after the cluster has disappeared. The vacancies and interstitials may then diffuse to sinks, i.e. lower energy locations in the crystal structure, and thereby form dislocations and dislocation loops. The dislocations may in turn grow three-dimensionally to form voids. Such voids will contribute to the volumetric swelling of the material due to the irradiation.

High energy neutrons can also generate other cavities in a material by gas formed in the material by nuclear reactions, i.e. n,p reactions, producing hydrogen, or n,alpha reactions, producing helium. The gas atoms can also diffuse to low energy locations and grow hydrogen and helium gas bubbles in the material. Such gas bubbles, when grown to sufficient size, will also contribute to the irradiation swelling and embrittlement of a material.

The formation of interstitials, vacancies, dislocations and voids can also lead to formation of secondary phases, which would otherwise not be formed without the microstructural change of the material.

The resulting microstructural changes discussed previously will depend on the material, some important impurities in the material, the fast neutron fluence, the temperature during irradiation and after the irradiation has ceased, and the time at temperature.

The microstructural changes can also result in changes in the mechanical properties of the material. Most materials are, for instance, hardened by irradiation. This means that the yield stress of the material will increase while the ductility, i.e. ability to deform plastically, will decrease. Void formation and precipitation of second phases can also lead to material embrittlement.

Transmutation is generally caused by thermal neutrons or absorption of epithermal neutrons due to resonance peaks. Transmutation will cause a chemical change in the material since a new chemical element is formed. Occasionally the transmutation reaction can also cause microstructural effects if the energy released during the neutron capture or a subsequent nuclear reaction has high energy. The new element can sometimes take the place of the mother element in the crystal lattice or form new phases if the solubility of the formed element is low or if the energy of formation has been lowered due to other microstructural changes by the fast neutron irradiation.

The thermal and epithermal neutrons do not directly contribute to the microstructural changes as described for fast neutrons. The new phases formed could, however, cause disturbance to the crystalline structure of a material, resulting in embrittlement and swelling, just as for fast neutrons, but obviously due to quite different causes.

4.4.3 Irradiation Effects in Tungsten

As discussed in section 4.4.2, irradiation effects from fast neutrons for tungsten will be as described for the materials in general. Details about the magnitude of the various effects are discussed in the following.

Pronounced absorption peaks are found in the epithermal absorption spectrum around 20 eV for tungsten, see section 3.6. The transmutation will lead to production of rhenium, Re, and some other products at lower concentrations, among them osmium, Os (Refs. 18, 24, 30, 32, 39).

A significant number of irradiation studies on tungsten have been reported, as shown by Table 4.4-1.

TABLE 4.4-1 IRRADIATIONS OF TUNGSTEN AND TUNGSTEN ALLOYS

a,c

Most of the studies, and especially those at higher fluences, have been performed in reactors with a pronounced fast flux, such as the FFTF, EBR-II and BOR-60. Irradiations in a predominantly fast flux will produce the microstructural changes discussed in Section 4.4.2, but the simultaneous transmutation, to rhenium and eventually osmium, will not have occurred to the same extent as would be experienced in a PWR core with similar fast flux fluence. However, a number of the studies with regard to the irradiation impact of neutrons on tungsten in Table 4.4-1 have been performed on W-Re alloys up to 26% Re, the solubility limit of rhenium in tungsten (see section 4.2.5). [

]a,c

[ ]^{a,c} Specific characteristics will be discussed in Section 4.4.5.

The irradiation temperature is important, mainly for the fast neutron impact, since a diffusion rate enhanced by elevated temperature during the irradiation will allow annealing of radiation effects such as vacancies and dislocations. An elevated temperature will also allow faster growth of voids and gas bubbles, i.e. increase swelling. As is seen in Table 4.4-1, a wide temperature range has been studied, along with the wide neutron fluence range, in the available neutron irradiation studies on tungsten.

4.4.4 Expected Limiting Fluences

[

]^{a,c}

[

]^{a,c}

4.4.5 Impact of Irradiation

In the application of tungsten in the enhanced GRCA design, the two potentially most significantly impacted properties by irradiation are ductility and swelling. These are discussed in the following sections. It should be noted that the double encapsulation feature of the enhanced GRCA design plays a key role in addressing the impact of these characteristics.

4.4.5.1 Mechanical Impact on Tungsten due to Irradiation

Neutron irradiation of tungsten will increase the ductile to brittle transition temperature (DBTT) of tungsten. This temperature, which is around room temperature for the unirradiated material depending on various metallurgical parameters, will increase significantly even after a low attained fluence of fast neutrons (Refs. 25, 47). The DBTT of tungsten was reported to change from 75°C to 880°C from unirradiated state to a fluence of 5.6×10^{21} n cm^{-2} (E>0.1 MeV) obtained at 300°C (Ref. 22). The increase of the DBTT occurs at lower fluences for W-Re alloys (Refs. 22, 25) although the DBTT is lowered for the unirradiated material by adding rhenium to the tungsten (Ref. 25).

The yield stress at 300°C was reported to decrease from 780 MPa to about 100 MPa by irradiation to $1x10^{21}$ n cm^{-2} neutron fluence (energy range unspecified) with no elongation and brittle fracture in a tensile test (Ref. 31). Further irradiation to $15x10^{21}$ n cm^{-2} lowered the yield stress to approximately 70 MPa in this study. In another study (Ref. 28), the yield stress was actually increased by irradiation to $9x10^{21}$ n cm^{-2} (E>0.1 MeV) in tensile tests at 427°C and an irradiation temperature of 382°C. Some ductility, well above 1%, remained in the material at these fluences.

The brittle cracking of the material seems to be both intergranular and transgranular at both low (Ref. 43) and high (Ref. 30) fast neutron fluences.

The variation in the results in the studies on the mechanical behavior implies that processing or maybe impurities of the tungsten will affect the embrittlement of the tungsten material. In some cases, rather good ductility can be obtained even at higher fluences while in at least one reported case, the embrittlement is rather pronounced.

As a consequence, it is considered that tungsten will become brittle even after a very short exposure (months) in a PWR neutron spectrum in the designed application as GRCA absorber material. Even so, the irradiation experience has shown that the irradiated pure tungsten will still be intact, i.e. obviously not powdered, allowing measurements of dimensions and performing immersion density determination of samples irradiated to $55x10^{21}$ n cm^{-2} (E>0.1 MeV) (Ref. 37) and even $144x10^{21}$ n cm^{-2} (E>0.1 MeV) (Ref. 30). In the latter case, the thin TEM samples occasionally broke during handling with tweezers. In another instance, TEM samples were manufactured from W-26%Re irradiated to $95x10^{21}$ n cm^{-2} (E>0.1 MeV) (Ref. 21), again showing that the material integrity is not jeopardized by even high fluences of fast neutrons. Although tungsten becomes brittle, the inner sleeve that provides double encapsulation serves to provide support for the tungsten such that the brittleness is directly considered in the design.

4.4.5.2 Swelling of Tungsten due to Irradiation

Swelling of tungsten has been studied at rather high fluences, up to $5.5x10^{22}$ n cm^{-2} neutron fluence (E>0.1 MeV). As expected, a notable effect of temperature was found and the maximum swelling was found at around 800°C, see Figure 4.4-1. [

]^{a,c} Note that this amount of swelling is much lower than that of other control rod absorber materials.

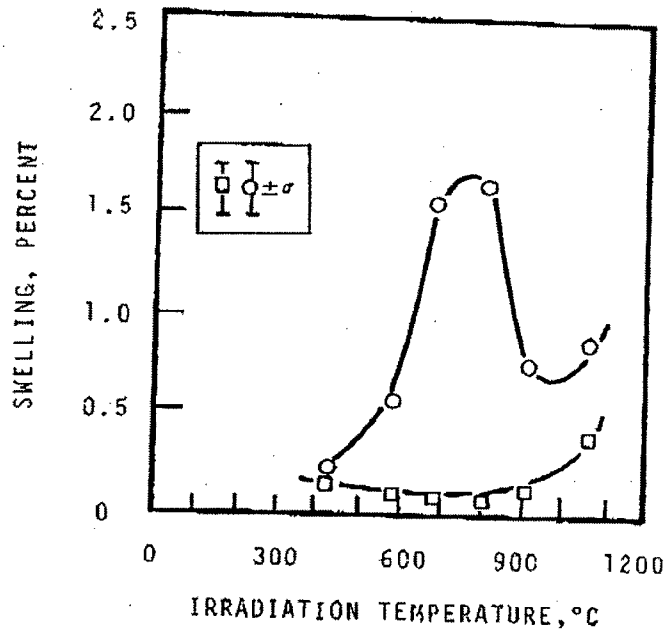

FIGURE 4.4-1 Swelling of tungsten (circles) and W-25%Re (squares) by immersion density measurement at a fluence of 5.5×10^{22} n cm^{-2} neutron fluence (E>0.1 MeV) (1×10^{22} n cm^{-2} neutron fluence (E>1 MeV)) in the EBR-II reactor (Ref. 37)

Irradiation of dynamically compacted tungsten, with a resulting density of 95.3%, to 14.4×10^{22} n cm^{-2} neutron fluence (E>0.1 MeV) at 600°C resulted in a densification of 2 to 3% rather than swelling (Ref. 35). This implies that the volumetric swelling for the dense tungsten material must be less than 3% even if we assume the swelling could perfectly fill all the voids present in the material originally. This is observed despite the very high fluence, which is almost three times higher than for the material in Figure 4.4-1. The calculated transmutation in this material, despite being exposed in a hard spectrum (Ref. 32), was found resulting in 1% rhenium and about 1% osmium and obviously these irradiation-created alloying elements do not significantly change the materials behavior. The rhenium and osmium were not found in the grain boundaries but seemed to be evenly distributed in the material (Ref. 35) as expected from the rather high solubility of Re and Os in body-centered-cubic tungsten and the substitutional nature of the alloy.

It is further shown in Figure 4.4-1 that the presence of rhenium, the main transmutation product of tungsten in a PWR spectrum, will decrease the swelling behavior in relation to pure tungsten. This is consistent with the observation that tungsten alloys with 25 to 26% rhenium do not exhibit any voids even at high fluences, i.e. 19×10^{21} n cm^{-2} (E>0.1 MeV) (Ref. 42) or more (Refs. 21, 38), although some voids were detected in one study (Ref. 49). The swelling of a W-25%Re material with a fluence of 37×10^{21} n cm^{-2} (E>0.1 MeV) irradiated at a temperature of 700°C to 900°C was reported to be less than 0.3% (Ref. 38), consistent with the data in Figure 4.4-1. The limited swelling actually recorded in the W-Re material has been reported to be due to precipitation of second phase particles due to the fast fluence (Ref. 38), which also explains a limited fluence and temperature impact on the W-Re alloy swelling below approximately 1000°C. In a tungsten alloy with 3% rhenium irradiated at 800°C, some voids were observed although less than in pure tungsten. No voids were observed in a W-26%Re alloy in the same study. The resulting swelling, evaluated from the microstructural measurements, was about 10 times lower in the W-3%Re alloy relative to the pure tungsten (Ref. 40). Voids were not found in a W-10%Re alloy irradiated to a fluence of 40×10^{21} n cm^{-2} (E>0.1 MeV) at 575°C to 675°C (Refs. 48, 49). The mitigating effect of rhenium on void formation in tungsten hence occurs in the range of 3 to 10% rhenium alloyed in the tungsten.

The results shown in Figure 4.4-1 are quite consistent with the general rule that swelling is not seen for materials at temperatures below $T < 0.3\ T_m$, i.e. temperatures below 30% of the melting temperature (on the Kelvin scale), since voids will not be formed below that temperature (Refs. 27, 29). Voids have, however, been observed in tungsten above 1000°C (1273 K) (Ref. 27).

Helium and hydrogen formation in tungsten from fast neutron impact is very limited compared with many other elements (Refs. 27, 33). Only about 0.2 appm of helium has been calculated to form in tungsten even with the 14 MeV high energy neutrons in the ITER design at a fluence of 2×10^{21} n cm^{-2} (Ref. 25). This very low helium, and hydrogen, formation is supported by calculations performed by Westinghouse, see section 3.6. In addition, a rather high temperature is needed to allow He diffusion and gas bubble formation in such a refractory material as tungsten (Ref. 29). Gas bubble formation will hence have negligible impact on the swelling for tungsten under irradiation in a PWR neutron spectrum relative to the void formation.

4.4.5.3 Tungsten Swelling from Transmutation

The formation of rhenium by transmutation of tungsten will have little effect on the structure of the tungsten since rhenium has a high solubility (more than 25%) in tungsten. The W-Re alloys within the solubility range also have a slightly higher density (Refs. 36, 38) and will not cause a swelling effect, contrary to what has been noted by phases formed by transmutation for Ag-In-Cd alloys at high neutron fluences. In addition, the presence of rhenium has been shown to impede the already limited fast neutron induced swelling in tungsten if alloyed (Ref. 37) as illustrated by the lower curve in Figure 4.4-1 and discussed above.

4.4.6 Summary of Material Property Impacts

1. Significant irradiation experience exists such that the impacts of irradiation on key characteristics of the GRCA design can be assessed under AP1000 operating conditions. Among the various studies conducted there is a strong consistency in the trends of the data.

2. In order to protect the tungsten against embrittlement and oxidation, the enhanced GRCA design will double encapsulate the tungsten absorber. The double encapsulation insures that no coolant will come into contact with the tungsten absorber even in the unlikely event of an outer cladding breach. The inner sleeve also serves to provide support for the tungsten under the effects of irradiation embrittlement.

3. Some limited swelling is expected for tungsten in a GRCA application. Swelling less than 0.7% diametral or axial elongation is inferred for fluence up to 55×10^{21} n cm^{-2} (E>0.1 MeV) from the published data. An absorber operating temperature below 800°C will lower the swelling rate further. The encapsulating internal sleeve is not required to have significant ductility or creep rate since only a very limited dimensional change will be experienced by the tungsten even at high fluences.

5.0 Design Bases and Evaluations

5.1 Nuclear Design

5.1.1 GRCA Reactivity Worth

Design Basis:

GRCAs shall have sufficient control rod worth over their life time such that they are capable of compensating for the intended reactivity effects as assumed in the plant's load follow operating strategy.

Evaluation:

Simulations of AP1000 load follow maneuvers down to 50% rated thermal power have established that GRCA bank worths of [ ]^{a,c} on average are ideal for meeting the operational requirement to perform such maneuvers without requiring a change in the core soluble boron concentration. The original approved four-rodlet Ag-In-Cd GRCA design was confirmed to provide this average targeted worth in actual core designs, and to meet the load follow operational requirement. The four-rodlet Ag-In-Cd design was therefore established as the basis for comparison with all other enhanced GRCA design concepts that were considered. The tungsten based enhanced GRCA design described in this report has been confirmed to meet the targeted GRCA control rod worth for AP1000, through comparison with the four-rodlet Ag-In-Cd GRCA design using unit assembly control rod worth calculations. This evaluation is described in Section 3.2.

5.1.2 GRCA Effect on Power Distribution

Design Basis:

Subject to meeting the minimum worth requirements in Section 5.1.1, GRCAs shall be designed to minimize the effect on core power distribution associated with their operation. This criterion helps to ensure that peaking factor limits can be met while maintaining an economical fuel management strategy, and also minimizes local pin power distribution effects in rodded assemblies.

Evaluation:

The tungsten based GRCA design described in this report has been confirmed to minimize both global and local effects on power distribution. This evaluation is described in Section 3.3.

5.2 Mechanical Design Bases and Evaluations

Design Basis:

For Conditions I and II, the stress and strain categories, and the strength theory presented in the ASME Code, Section III, are used as a general guide in the design of the GRCA structural parts. For conditions III and IV, code stresses are not limiting.

The design conditions considered under the ASME Code, Section III, are as follows:

- External pressure equal to the reactor coolant system operating pressure with appropriate allowance for overpressure transients
- Wear allowance equivalent to 1,000 reactor trips
- Bending of the rod due to a misalignment in the guide thimble
- Forces imposed on the rods during rod drop
- Loads imposed by the accelerations of the control rod drive mechanism
- Radiation exposure during maximum core life.
- Temperature effects at operating conditions.

In addition to meeting the above ASME conditions, specific enhanced GRCA evaluations are provided in the folowing Sections 5.2.1, 5.2.2, 5.2.3, and 5.2.4.

5.2.1 Internal Pressure and Cladding Stresses during Normal, Transient, and Accident Conditions

The design of GRCA rods provides a sufficient cold void volume to accommodate the minor internal pressure increase during operation. Very little gas is released by the tungsten absorber. Sufficient diametral and end clearances have been provided to accommodate the relative thermal expansion between the sleeve and the surrounding clad and end plugs. Thermal expansion of the sleeve and cladding is greater than that of the tungsten absorber.

GRCA rodlet and fuel assembly guide thimble and dashpot analyses indicate that the flow is sufficient to prevent coolant boiling within the guide thimble. Therefore, clad temperatures at which the clad material has adequate strength to resist coolant operating pressures are maintained.

5.2.2 Irradiation Stability of the Absorber Material, Taking into Consideration Gas Release and Swelling

The irradiation stability of the tungsten absorber material is discussed in Section 4.4.5.1. Irradiation produces no deleterious effects in the absorber material. Some minor cracking of the tungsten material may occur, but this cracking does not affect the absorber column geometric stability, due to the very small diametral clearance between absorber and sleeve in operation.

As previously mentioned, gas release is not a concern for the gray control rod material because very little gas is produced by the absorber material.

5.2.3 Absorber Material Swelling

The irradiation swelling of tungsten material is discussed in Sections 4.4.5.2 and 4.4.5.3. Sufficient diametral and end clearances have been provided to accommodate the absorber volumetric swelling and the relative thermal expansion between the sleeve and the surrounding cladding and end plugs, such that the cladding will not be mechanically loaded due to absorber swelling. The small amount of tungsten swelling noted in Section 4.4.6 is also accommodated by the inner sleeve [

]a,c

5.2.4 Potential for Interaction Between the Absorber and the Coolant

As discussed in Section 4.3, tungsten is subject to oxidation if it comes into contact with the reactor coolant. However, the double encapsulation feature of the enhanced GRCA rodlet design provides additional protection. Even in the highly unlikely event of a breach of the outer cladding, the inner sleeve will provide protection for the tungsten absorber.

5.3 Thermal and Hydraulic Design Bases and Evaluation

The GRCA is operated at various insertion elevations into the core, from fully inserted to fully withdrawn. The limiting condition for thermal calculations is when the GRCA is fully inserted and the core is at 100% power. Long-term power shapes are of interest for determining the operating temperature of the GRCA components as well as defining the heating rate for boiling criteria evaluations. In addition, all normal operation (Condition I) or upset (Condition II) conditions need to be evaluated to determine the maximum GRCA temperatures.

The rodlet linear heating rate of the GRCA is a key parameter in the thermal evaluations. This includes the heating of the tungsten absorber, the sleeve, and the cladding. Compared to a typical RCCA (silver-indium-cadmium), the enhanced GRCA has a lower rodlet heating rate by approximately 40%.

The following sections provide a summary of the thermal and hydraulic design bases and the associated evaluations performed using the standard Westinghouse design and analysis methodology for the these types of in-core components. Appropriate heating rates are use to reflect the incorporation of the tungsten absorber in the GRCA design.

5.3.1 Maximum Absorber Temperature

Design Basis:

The maximum temperature of the absorber material shall not exceed its melting temperature during normal operation (Condition I) or an upset (Condition II) conditions. The melting temperature of Tungsten is approximately 3380 °C (> 6000 °F) as stated in Section 4.1.1.

Evaluation:

The maximum absorber temperature was calculated using maximum $F_{\Delta h}$, maximum fuel rod F_Q, and overpower conditions (Condition II). This provides the maximum local heating in the absorber, thus resulting in the maximum temperature. Thermal evaluation shows that the maximum absorber temperature is much less than the tungsten melting temperature. Likewise, the maximum sleeve and cladding temperatures are much lower than the melting temperature of the respective materials.

In addition to maintaining the temperatures below the material melting temperature for maximum heating during Condition II conditions, it is desirable to maintain relatively low GRCA temperatures during normal, long-term operation (Condition I). Therefore, the GRCA rodlet design has features that are used to keep the operating temperature as low as possible. The gaps between the cladding, sleeve, and absorber are minimized as much as practical to reduce the temperature increase across them. In addition, helium gas is used instead of air in the largest gap, which is the cladding-to-sleeve gap. Helium has a higher thermal conductivity than air, thus improving the heat transfer and reducing the temperature rise across this gap.

To calculate realistic operating temperatures, the local power suppression in the GRCA rodlet due to presence of the absorber is considered. Therefore, the calculation of operating temperatures utilizes lower local values than maximum $F_{\Delta h}$ and maximum fuel rod F_Q.

Thermal-hydraulic analysis has shown that the criterion of maximum temperature of the absorber material not exceeding its melting temperature is met for this GRCA design.

5.3.2 No Surface Boiling within the Dashpot Region

Design Basis:

During normal operation (Condition I), there will be no surface boiling on the absorber cladding in the dashpot region.

Evaluation:

The flow in the dashpot is much lower than the flow in the guide thimble tube above the dashpot, where side holes in the guide thimble tube inject more coolant into this tube. Therefore, the temperature conditions in the dashpot need to be evaluated.

The GRCA utilizes [

]^{a,c} This is the only portion of the GRCA that is in the dashpot, and this only occurs when the GRCA is inserted deeply into the fuel assembly. The limiting condition for surface boiling on the absorber cladding is when the GRCA is fully inserted in the fuel assembly, and this condition was evaluated.

Thermal-hydraulic analysis has shown that this criterion of no surface boiling on the absorber cladding is met for this GRCA design.

5.3.3 No Bulk Boiling in the Guide Thimble Tubes

Design Basis:

During normal operation (Condition I), there will be no bulk boiling in the guide thimble tubes.

Evaluation:

Like the dashpot region evaluation, the limiting condition is when the GRCA is fully inserted into the fuel assembly. The flow in the guide thimble tubes is much higher than the flow in the dashpot region. However, the temperature of this tube flow increases with increasing elevation in the core so the temperature conditions in the guide thimble tube need to be evaluated.

Thermal-hydraulic analysis has shown that the no bulk boiling in the guide thimble tubes criterion is met for this GRCA design.

5.3.4 Bypass Flow in Guide Thimble Tubes

Design Basis:

The core bypass flow through the guide thimble tubes is limited to assure that sufficient coolant flow is provided to the fuel rod channels to meet fuel and thermal hydraulic design criteria. The maximum guide thimble tube bypass flow, when combined with the other bypass flow paths in the reactor (see Section 4.4.4.2.1 of the DCD, Rev. 16), must be maintained below 5.9% of the overall core flow.

Evaluation:

Section 4.4.4.2.1 of the DCD, Rev. 16, has shown that the core bypass is no greater than 5.9% for calculations using worst case drawing tolerances and uncertainties in pressure losses. This GRCA design has no impact on these calculations. Therefore, this bypass flow criterion is met.

5.4 Summary

The principal difference between the Enhanced GRCA and current GRCA design described in DCD Chapter 4 is the tungsten absorber material. The Enhanced GRCA rodlet design is not significantly changed other than the substitution of the tungsten absorber material and the associated double encapsulation, as noted in Section 1.0. Evaluations have been performed to verify that the current approved/licensed DCD GRCA design bases and design criteria continue to be met for the enhanced GRCA design. The enhanced GRCA design has been evaluated using the NRC-approved Westinghouse methods consistent with the guidance in SRP 4.2.

6.0 Post-LOCA Survivability

An assessment of the enhanced GRCA was made regarding post-LOCA survivability for control rods to assure that this new design is no more limiting than the Rod Cluster Control Assembly (RCCA) or the previous GRCA. The primary issue is the potential formation of a eutectic between the stainless steel clad and the zirc-based thimble tube that would lower the melting point of the cladding and cause melting of the control rod design. The same materials are utilized and [ ]^{a,c}. Thus, the assessment performed for the RCCA in PA-ASC-0313, "Assessment of Post LOCA Control Rod Survivability," bounds the GRCA design and the GRCA design is acceptable.

An assessment was also made of the potential formation of low-temperature melting eutectics between the tungsten and the structural material. Phase diagrams for combinations of tungsten with iron and nickel, the main components in stainless steel and nickel-base materials, respectively, show that there are no such concerns for tungsten. The phase diagrams for tungsten and iron as well as for tungsten and nickel are not exhibiting any such low-temperature melting phases, as illustrated by Figure 6.0-1 and Figure 6.0-2.

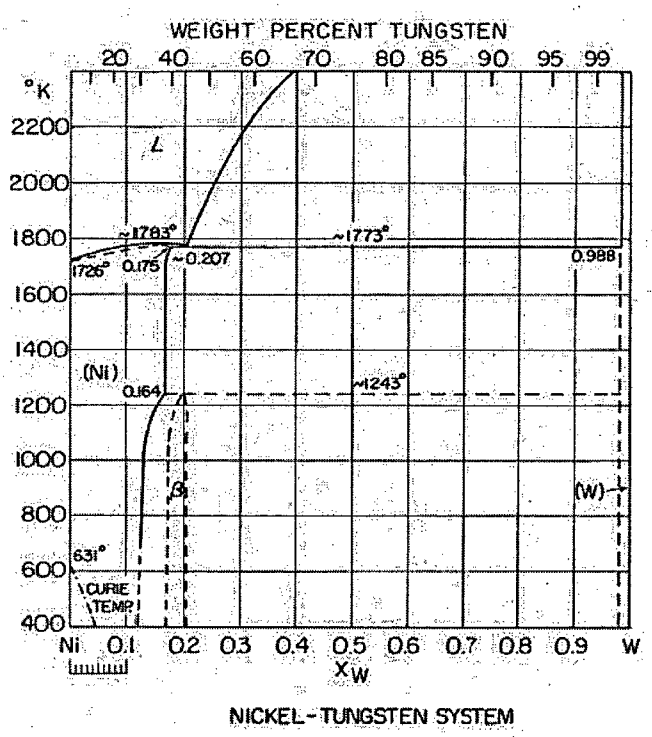

FIGURE 6.0-1 TUNGSTEN-NICKEL PHASE DIAGRAM (REFERENCE 12)

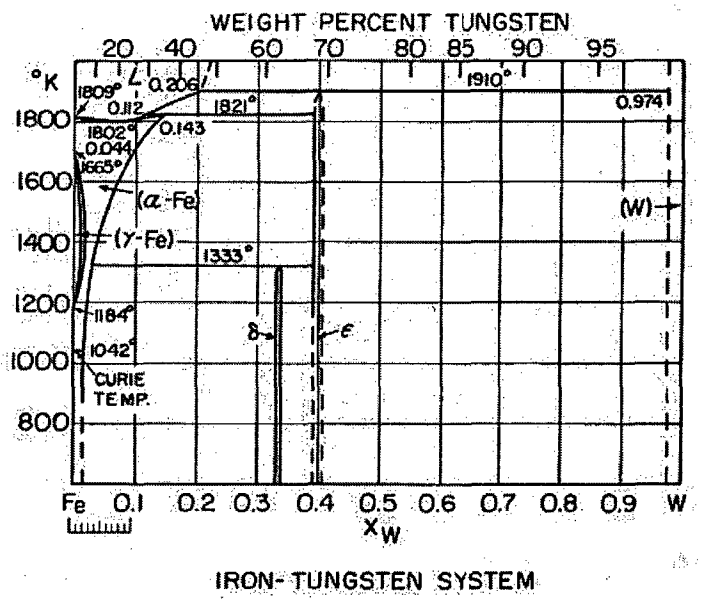

FIGURE 6.0-2 TUNGSTEN-IRON PHASE DIAGRAM (REFERENCE 12)

7.0 Operational Monitoring Program

In order to validate the expected performance of the enhanced GRCA design in the reactor core, Westinghouse will monitor specific aspects of the design over its lifetime. This approach will provide assurance that continuing successful performance is achieved and also identify any unforeseen issues in a timely fashion.

The two basic aspects of this approach include startup physics testing, as well as post-irradiation examination of the hardware itself.

Although there are no specific drop time requirements for the GRCAs (i.e. their insertion is not required to assure safe shut down of the reactor), rod drop testing will be routinely conducted, similar to that conducted for RCCAs, to track and identify any trends that might indicate adverse impacts on the GRCA design.

With regard to startup physics testing, GRCA bank worths will be measured each cycle during the beginning of cycle startup in the same manner as other control rod banks. The measurement of GRCA bank worth will confirm the adequacy of the nuclear design calculation methods and provide data to support improvements in future cycles, if necessary.

With regard to post-irradiation examination, pool-side and hot cell exams will be planned at specific points in the lifetime of the GRCA from a lead plant. In order to establish a baseline for PIE exams, selected GRCAs will be pre-characterized during the manufacturing process prior to shipment. A visual exam will be performed at an appropriate point after the first or second cycle. The purpose of the visual exams will be to identify any characteristics that may indicate adverse performance. Key areas of interest include cladding wear and any changes in cladding diameter, e.g. due to swelling. It should be noted that these mechanical and material attributes generally take place slowly over time. Based on the results of the early life visual exams and drop testing trends, subsequent visual exams, more detailed non-destructive exams and a hot cell exam will be planned at appropriate points in the lifetime of the GRCA. The non-destructive exams will provide more detailed information regarding wear and any other changes to the cladding. The hot cell exam will also provide information regarding the conditions inside the rod, including the performance of the tungsten absorber material and the sleeve. A factor in determining the timing of the hot cell exam will be the desire to obtain these detailed measurements at a time that will provide the best indication of integrated lifetime performance, while validating that ongoing experience meets the expected performance.

8.0 References

1. "AP1000 Design Control Document," Revision 15, November 2005

2. "AP1000 Design Control Document," Revision 16, May 2007

3. WCAP-16045-P-A, "Qualification of the Two-Dimensional Transport Code PARAGON," Ouisloumen M., et al, August 2004

4. WCAP-10965-P-A, "ANC: A Westinghouse Advanced Nodal Computer Code," Liu Y. S., et al, September 1986

5. ORNL/TM-2005/39, Version 5, Section F7, "ORIGEN-S: Scale System Module to Calculate Fuel Depletion, Actinide Transmutation, Fission Product Buildup and Decay, and Associated Radiation Source Terms," Gaud I. C., et al

6. LA-UR-03-1987, "MCNP – A General Monte Carlo N-Particle Transport Code, Version 5," April 24, 2003 (Revised 10/3/05)

7. KAPL-P-000069, "Neutron Total and Capture Cross Section Measurements of Tungsten," Werner C. J., et al, June 1998

8. NUREG-0800 Standard Review Plan, Section 4.2, Revision 3, "Fuel System Design," March 2007

9. Metals Handbook, 9th Ed., Vol. 2, p 816 – 821, American Society for Metals

10. Metals Handbook, 9th Ed., Vol. 3, p 348 – 349, American Society for Metals

11. R. Hultgren et al., *Selected Values of the Thermodynamic Properties of the Elements*, Metals Park, Ohio: Amer. Soc. Metals, 1973. p 547 – 551

12. R. Hultgren et al., *Selected Values of the Thermodynamic Properties of Binary Alloys*, Metals Park, Ohio: Amer. Soc. Metals, 1973, p 1299

13. Not used

14. Not used

15. O. Kubaschewski, E. Ll. Evans, and C.B. Alcock, *Metallurgical Thermochemistry*, 4th ed., Oxford: Pergamon Press, 1967, p 408

16. Y. Ishijima et al. *Journal of Nuclear Materials* 307–311 (2002) 1369–1374

17. *Tungsten* Plansee Product Literature

18 G.A. Cottrell, R. Pampin, N.P. Taylor. "Transmutation and Phase Stability of Tungsten Armor in Fusion Power Plants." *Fusion Science and Technology* Vol. 50 July 2006 89-98

19. F.W. Wiffen. "Effects of Irradiation on Properties of Refractory Alloys with Emphasis on Space Power Reactor Applications." in R.H. Cooper, Jr., and E.E. Hoffman, eds., Refractory Alloy Technology for Space Nuclear Power Applications, Proceedings of a symposium held at Oak Ridge, Tennessee, August 10-11, 1983. CONF-8308130 (DE84001745) Published by Technical Information Center, Office of Scientific and Technical Information, US Department of Energy, January 1984.

20. M. Kangilaski. "Radiation Effects Design Handbook." National Aeronautics and Space Administration, Washington D.C. October 1971

21. Yoshiyuki Nemoto, Akira Hasegawa, Manabu Satou, and Katsunori Abe. "Microstructural development of neutron irradiated W-Re alloys." *Journal of Nuclear Materials* 283-287 (2000) 1144-1147

22. Peter Krautwasser, Heinz Derz, and Erich Kny. "Influence of fast neutron fluence on the ductile-brittle transition temperature of Tungsten, W-10Re, and W-3.4Ni" *12th International Plansee Seminar* '89.vol 22 number 1 (1990) 25-32

23. G.M. Kalinin. "High-Z plasma-facing and related materials." *Journal of Nuclear Materials* 179-181 (1991) 1193-1198

24. C.B.A. Forty, G.J. Butterworth, J.-Ch. Sublet. "Burnup of some refractory metals in a fusion neutron spectrum." *Journal of Nuclear Materials* 212-215 (1994) 640-643

25. V. Barabash et al. "Neutron irradiation effects on plasma facing materials." *Journal of Nuclear Materials* 283-287 (2000) 138-146

26. I. Smid et al. "Development of tungsten armor and bonding to copper for plasma-interactive components." *Journal of Nuclear Materials* 258-263 (1998) 160-172

27. R.C. Rau, R.L. Ladd, and J Moteff. "Voids in Irradiated Tungsten and Molybdenum." *Journal of Nuclear Materials* 33 (1969) 324-327

28. J.M. Steichen. "Tensile properties of neutron irradiated TZM and tungsten." *Journal of Nuclear Materials* 60 (1976) 13-19

29. H. Ullmaier, F. Carsughi. "Radiation damage problems in high power spallation neutron sources." *Nuclear Instruments and Methods in Physics Research B* 101 (1995) 406-421

30. L.R. Greenwood, F.A. Garner. "Transmutation of Mo, Re, W, Hf, and V in various irradiation test facilities and STARFIRE." *Journal of Nuclear Materials* 212-215 (1994) 635-639

31. I.V. Gorynin. "Effects of neutron irradiation on properties of refractory metals." *Journal of Nuclear Materials* 191-194 (1992) 421-425

32. L.R. Greenwood, F.A. Garner. "Impact of transmutation issues on interpretation of data obtained from first fast reactor irradiation experiments." *Journal of Nuclear Materials* 329-333 (2004) 1147-1150

33. V. Barabash et al. "Material/plasma surface interaction issues following neutron damage." *Journal of Nuclear Materials* 313-316 (2003) 42-51

34. M. Ekman, K. Persson, G. Grimvall. "Phase diagram and lattice instability in tungsten-rhenium alloys." *Journal of Nuclear Materials* 278 (2000) 273-276

35. J. Megusar, F.A. Garner. "Response of dynamically compacted tungsten to high fluence neutron irradiation at 423-600°C in FFTF." *Journal of Nuclear Materials* 258-263 (1998) 940-944

36. M. Fujitsuka, B. Tsuchiya, I. Mutoh, T. Tanabe, T Shikama. "Effect of neutron irradiation on thermal diffusitivity of tungsten-rhenium alloys." *Journal of Nuclear Materials* 283-287 (2000) 1148-1151

37. J. Matolich, H. Nahm, and J. Moteff. "Swelling in neutron irradiated tungsten and tungsten-25 percent rhenium." *Scripta Metallurgica* Vol. 8 No.7 (1974) 837-842

38. R.K. Williams, F.W. Wiffen, J. Bentley, and J.O. Stiegler. "Irradiation Induced Precipitation in Tungsten Based, W-Re Alloys." *Metallurgical Transactions A* Vol. 14A April 1983 655-666

39. R. Pampin. "Tungsten transmutation and resonance self-shielding in PPCS models for the study of sigma-phase formation." Euratom/UKAEA Fusion October 2005

40. J.C. He, G.Y. Tang, A. Hasegawa, and K. Abe. "Microstructural development and irradiation hardening of W and W-(3-36)wt% Re alloys after high-temperature neutron irradiation to .15dpa." *Nucl. Fusion* 46 (2006) 877-883

41. L.K Keys, J.P. Smith, and J. Moteff. "High-Temperature Recovery of Tungsten after Neutron Irradiation." *Nuclear Systems Programs* Volume 176 number 3, 15 December 1968

42. V.K. Sikka and J.Moteff. "Identification of a-Mn Crystle Structure in Neutron Irradiated W-Re Alloy." *Metallurgical Transactions* Volume 5 June 1974 1514-1517

43. Younger and Wright., NASA Tech Note TN D-5991, 1970

44. Yih, et al, *Tungsten: Sources, Metallurgy, Properties and Applications*, Plenum Press 1979.

45. Greene and Finfrock, BNL Formal Report BNL-52621, Oct. 2000

46. Riech, *Tungsten and its Compounds*, Pergamon Press 1967

47. Erik Lassner, and Wolf-Dieter Schubert. Tungsten, Properties, Chemistry, Technology of the Element, Alloys, and Chemical Compounds. (1999) 85-155

48. R. Herschitz and D.N. Seidman, "Overview No. 39, An Atomic Resolution Study of Homogeneous Radiation-Induced Precipitation in a Neutron Irradiated W-10at% Re Alloy," *Acta Metall.* 32, 8, p.1141-1154 (1984)

49. Roman Herschitz and David N. Seidman, "Radiation-Induced Precipitation in Fast-Neutron Irradiated Tungsten-Rhenium Alloys: an Atom-Probe Field-Ion Microscope Study," *Nuclear Instruments and Methods in Physics Research* B7/8 (1985) p.137-142